Received: 21 November 2018 | Revised: 28 May 2019 | Accepted: 3 June 2019

DOI: 10.4218/etrij.2018-0662

FEATURED ARTICLE

ETRI Journal WILEY

Millimeter-wave directional-antenna beamwidth effects on the ITU-R building entry loss (BEL) propagation model*

Juyul Lee[1] | **Kyung-Won Kim**[1] | **Myung-Don Kim**[1] | **Jae-Joon Park**[1] | **Young Keun Yoon**[2] | **Young Jun Chong**[2]

[1]Hyper-connected Communication Research Laboratory, Electronics and Telecommunications Research Institute, Daejeon, Rep. of Korea

[2]Broadcasting Media Research Laboratory, Electronics and Telecommunications Research Institute, Daejeon, Rep. of Korea

Correspondence
Juyul Lee, Hyper-connected Communication Research Laboratory, Electronics and Telecommunications Research Institute, Daejeon, Rep. of Korea.
Email: juyul@etri.re.kr

Funding information
This research was supported by the Institute for Information & communications Technology Promotion (IITP) grant funded by the Korean government (MSIT) [2017-0-00066, "Development of time-space based spectrum engineering technologies for the preemptive using of frequency."

Assuming omnidirectional antenna reception, the ITU-R recently developed a new propagation model on building entry loss (BEL) for 5G millimeter-wave frequency sharing and compatibility studies, which is a simplified outdoor-to-indoor path loss model. Considering the utilization of high-gain narrow-beamwidth beamforming, the omnidirectional-based ITU-R BEL model may not be appropriate to predict propagation characteristics for directional beamforming scenarios. This paper studies the effects of beamwidth on the ITU-R BEL model. This study is based on field measurements collected with four different beamwidth antennas: omnidirectional, 10° horn, 30° horn, and 60° horn. The measurement campaigns were conducted at two types of building sites: traditional and thermally efficient buildings. These sites, as well as the measurement scenarios, were carefully chosen to comply with the ITU-R BEL measurement guidelines and the ITU-R building types. We observed the importance of accurate beam alignment from the BEL variation range. We were able to quantify the beamwidth dependency by fitting to a model that is inversely proportional to the beamwidth.

KEYWORDS
beamforming, channel model, outdoor-to-indoor propagation, path loss

1 | INTRODUCTION

In the course of new spectrum allocation for 5G millimeter-wave (mmWave) systems, the ITU-R has been conducting a frequency sharing and compatibility study since 2015 [2]. To provide guidance, the ITU-R released a new recommendation in 2017 on a *building entry loss* (BEL) propagation model, which is a simplified outdoor-to-indoor (O2I) path loss model [3,4].

The ITU-R BEL model was developed only for omnidirectional antenna reception; however, narrow-beamwidth directional beamforming will most likely be used to overcome the severe free space loss at mmWave frequencies. It is known that the propagation characteristics captured with a narrow-beamwidth antenna are different from those captured with an omnidirectional antenna, especially in multipath-rich environments due to spatial filtering effects [5], and therefore, the BEL model

*An initial study of this paper was presented at the 2018 Global Symposium on Millimeter Waves (GSMM), Boulder, CO, May 2018 [1]. It should be noted that the initial study was conducted with different measurement data.

will be affected when receiving with a narrow-beamwidth antenna since receivers are typically located in multipath-rich indoor environments. In this paper, we empirically analyze the effect of antenna beamwidth on the ITU-R BEL model.

We conducted measurement campaigns at the 32-GHz band, which is one of the 5G mmWave candidate frequency bands [2], at two different building sites. These sites were carefully selected to comply with the ITU-R building-type classification. It should be noted that there are only two building-type classes in the ITU-R standard [3]. Although there were numerous debates on the building classification during the ITU-R standardization process, it was decided to use a simple dichotomy—differentiating between traditional type and thermally efficient type, depending on the existence of thermal-efficiency window materials [6]. That is why our measurement campaigns were conducted at these two building sites. To investigate the antenna beamwidth effect on the BEL, our measurements were obtained with several different beamwidth antennas and were analyzed using beamwidth synthesis techniques. The TX was fixed (outside the building) and pointed perpendicularly to the building, while maintaining a clear line-of-sight from the TX to the building facade. The RX was moved, to the extent possible, uniformly within the building, as per the ITU-R measurement guideline [7].

To the best of our knowledge, the O2I propagation measurements date back to 1959 [8], in which the building penetration losses at 35 MHz and 150 MHz were reported to be 20 dB–25 dB on average. Since then, the O2I propagation characteristics have been studied in various aspects and frequency bands below 6 GHz [9–11] (and references therein). Most of them were concerned with building penetration losses as a function of building materials and structures. In addition, the recently published [12–16] reported the O2I characteristics for mmWave frequency bands. Based on these studies, including [17], COST 231 [18], WINNERs [19,20], 3GPP [21], and ITU-R (Study Group 5), [22] adopted the O2I propagation characteristics in their standard specifications. Independently, another group in the ITU-R (Study Group 3) [3] recently released O2I propagation loss characteristics and named it BEL. However, as noted above, all of these reports including [3] do not consider the impact of antenna beamwidth. This may provide unrealistic predictions when a directional high-gain narrow-beamwidth reception is employed in multipath-rich indoor environments. In our prior conference publication [1], we initially investigated the same issue, namely impact of beamwidth on the BEL, based on the measurements conducted at one TX location only. Although the general conclusion is similar, the statistics (from empirical analysis) may not be accurate since the prior work was investigated with only a limited dataset. In this work, however, we have tried to collect sufficient measurement data (by varying the TX locations and RX location uniformly in the building) to perform an improved statistical analysis and provide more solid results.

2 | PRELIMINARIES

To begin with, we briefly review the ITU-R BEL model [3], which was developed by the ITU-R Study Group 3 (Propagation). Note that there is another ITU-R group (Study Group 5), which developed an O2I model [22,23] that is similar to the 3GPP O2I model [21]. Besides these, there are other standardized models such as COST 231 [18] and WINNERs [19,20], which are also similar to the 3GPP model. Therefore, along with the ITU-R BEL, we also review the 3GPP O2I model in this section.

2.1 | The ITU-R BEL model

The ITU-R defines the BEL as "the additional loss due to a terminal being inside a building" [7], in which the details of measurement guidance are also provided. Based on the theoretical definition and the measurement guidelines, the ITU-R gathered over 6000 measurement data points on 40 frequency bands and discussed how the model should be parameterized, in order to develop appropriate propagation models for frequency sharing and compatibility studies for 5G mmWave bands [3,24]. The BEL model was decided to be a statistical model considering "equal probability of location at any point within a building" without assuming a specific TX and RX arrangement with respect to a building [3]. By compiling the measurement data and harmonizing various opinions, it was decided to divide buildings into two classes, namely "traditional buildings" and "thermally efficient buildings," which can be determined from the building materials and not from the actual construction year [3,4]. Regarding the incidence angles to the building, only the elevation angle dependency was considered [3]. The current version of the ITU-R standard considers only clear line-of-sight from the TX to the building facade [3], while cluttered BEL (ie, combining clutter loss and BEL) is left to a future work.

Based on the harmonization, the ITU-R released its first version of the BEL model in Recommendation ITU-R P.2109 in 2017, which is valid for frequencies between 80 MHz and 100 GHz, in a cumulative distribution function for the probability p ($0 < p < 1$) [3]:

$$L_{\text{ITU-R\_BEL}}(p) = 10\log_{10}\left(10^{0.1A(p)} + 10^{0.1B(p)} + 10^{0.1C}\right)(\text{dB}), \quad (1)$$

where

$$A(p) = F^{-1}(p)\sigma_1 + \mu_1, \quad (2)$$

$$B(p) = F^{-1}(p)\sigma_2 + \mu_2, \quad (3)$$

$$C = -3.0, \quad (4)$$

$$\mu_1 = L_h + L_e, \tag{5}$$

$$\mu_2 = w + x \log_{10} f, \tag{6}$$

$$\sigma_1 = u + v \log_{10} f, \tag{7}$$

$$\sigma_2 = y + z \log_{10} f, \tag{8}$$

where f is the operating frequency in GHz, $F^{-1}(p)$ is the inverse cumulative normal distribution, and L_h is the median loss for the horizontal paths, which is given by

$$L_h = r + s \log_{10} f + t(\log_{10} f)^2, \tag{9}$$

and L_e is the correction for the elevation angle θ of the path at the building facade given by $L_e = 0.212|\theta|$. All the parameters for the traditional and thermally efficient buildings are listed in Table 1. Further details about the ITU-R BEL model are referred to [3] and some measurement information used to derive the model can be found in [24].

2.2 | The 3GPP O2I Model

Likewise, the 3GPP provides O2I building penetration loss characteristics in its standard TR 38.901 [21]:

$$L_{3GPP\_O2I} = L_b + L_{tw} + L_{in} + \mathcal{N}(0, \sigma_P^2) \tag{10}$$

where L_b is the basic outdoor path loss, L_{tw} is the building penetration loss, L_{in} is the building inside loss, and $\mathcal{N}$ denotes the normal distribution with the variance σ_P^2. Compared to the ITU-R BEL, the last three additive terms in (10) correspond to the building entry loss, That is,

$$L_{3GPP\_BEL} = L_{tw} + L_{in} + \mathcal{N}(0, \sigma_P^2), \tag{11}$$

TABLE 1 ITU-R BEL model parameters [3]

Parameter	Traditional building	Thermally efficient building
r	12.64	28.19
s	3.72	−3.00
t	0.96	8.48
u	9.6	13.5
v	2.0	3.8
w	9.1	27.8
x	−3.0	−2.9
y	4.5	9.4
z	−2.0	−2.1

where

$$L_{tw} = L_{npi} - 10 \log_{10} \sum_{i=1}^{N} \left(p_i \times 10^{\frac{L_{material\_i}}{-10}} \right), \tag{12}$$

where L_{npi} denotes the additional loss for the nonperpendicular incidence (however, no further description can be found in [21]) and p_i is the proportion ratio of the i-th material such that $\sum_{i=1}^{N} p_i = 1$. Unlike the ITU-R BEL model, the 3GPP O2I model can include various building material loss characteristics as follows:

$$L_{material\_i} = a_{material\_i} + b_{material\_i} \cdot f, \tag{13}$$

where $a_{material\_i}$ and $b_{material\_i}$ are material-dependent constants, for example, $L_{glass} = 2 + 0.2f$ for standard multipane glass, $L_{IRR\_glass} = 23 + 0.3f$ for IRR glass, and $L_{concrete} = 5 + 4f$ for concrete [21].

The 3GPP O2I model provides two exemplary cases for low-loss and high-loss models by (14) and (15), respectively, where $d_{2D\text{-}in}$ is the minimum of two uniform random variables between 0 and 25 m for urban cases.

$$L_{3GPP\_BEL,Low\text{-}loss} = 5 - 10 \log_{10} \left(0.3 \cdot 10^{\frac{L_{glass}}{-10}} + 0.7 \cdot 10^{\frac{L_{concrete}}{-10}} \right) + 0.5 d_{2D\text{-}in} + \mathcal{N}(0, 4.4^2), \tag{14}$$

$$L_{3GPP\_BEL,High\text{-}loss} = 5 - 10 \log_{10} \left(0.7 \cdot 10^{\frac{L_{IIR\_glass}}{-10}} + 0.3 \cdot 10^{\frac{L_{concrete}}{-10}} \right) + 0.5 d_{2D\text{-}in} + \mathcal{N}(0, 6.5^2) \tag{15}$$

Although a direct comparison between the ITU-R BEL model and the 3GPP model is difficult, since the building materials and the building types are not compatible, Figure 1 shows a comparison of the two models when the operating frequency is set to 32 GHz. It can be seen that the ITU-R models have wider BEL ranges, although the median values are similar (the max difference between the ITU-R BEL traditional model and the 3GPP O2I BEL low-loss model is about 2 dB). Note that [25] also deals with O2I model comparisons including the ITU-R and the 3GPP O2I models. However, their ITU-R model is from [22] (developed by Study Group 5), and not from [3] (developed by Study Group 3). It should be noted that the model developed by Study Group 5 is a simple variation of the 3GPP model, whereas Study Group 3 developed their model from scratch by gathering numerous measurement data [3,24].

3 | MEASUREMENT OVERVIEW

We built a 32-GHz mmWave wideband channel sounder (center frequency of 32.4 GHz and bandwidth of 500 MHz) by adding new RF parts to the existing base-band and IF parts

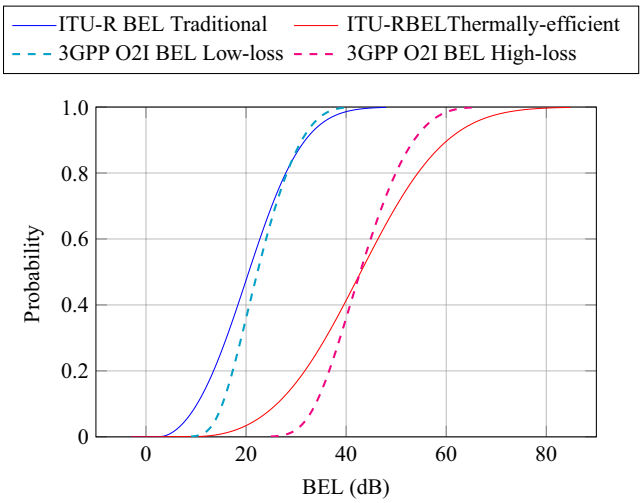

FIGURE 1 Comparison between the ITU-R BEL model and the 3GPP O2I BEL model when the operating frequency is 32 GHz

TABLE 2 RX Antenna gain

Antenna (HPBW)	Antenna gain (dBi)
10°-horn antenna	27.0
30°-horn antenna	15.6
60°-horn antenna	9.7
Omnidirectional antenna	5.8

of the 28- and 38-GHz sounders [26] (details about the other sounder specifications can be obtained from [26]). By using this 32-GHz sounder, our BEL measurements were conducted with four antennas (listed in Table 2) at the RX to investigate the antenna beamwidth[1] effect.

The BEL measurement campaigns were conducted in two ETRI office buildings (denoted by Building A and Building B) as shown in Figure 2. These buildings were initially constructed with similar concrete/windows and similar indoor structures. However, the exterior of Building B was recently renovated with metal-coated dual-layer windows, while the interior was unchanged. According to the ITU-R building-type classification [3], Building A is classified as a traditional type and Building B is classified as a thermally efficient type. As can be seen in Figure 2, Building A has six stories and Building B has five stories. The planar dimensions are 72 m × 25 m and 58 m × 27 m for Building A and Building B, respectively.

As shown in Figure 2, there are trees in front of the buildings, which can clutter the TX signals. To avoid such clutter and other obstacles between the TX and the building facade, we installed the TX antenna high on a lift as illustrated in Figure 2. The measurement guide in the current ITU-R Recommendation [7] requires a clear line-of-sight condition

[1]Throughout the paper, the beamwidth is calculated using the half-power beamwidth (HPBW).

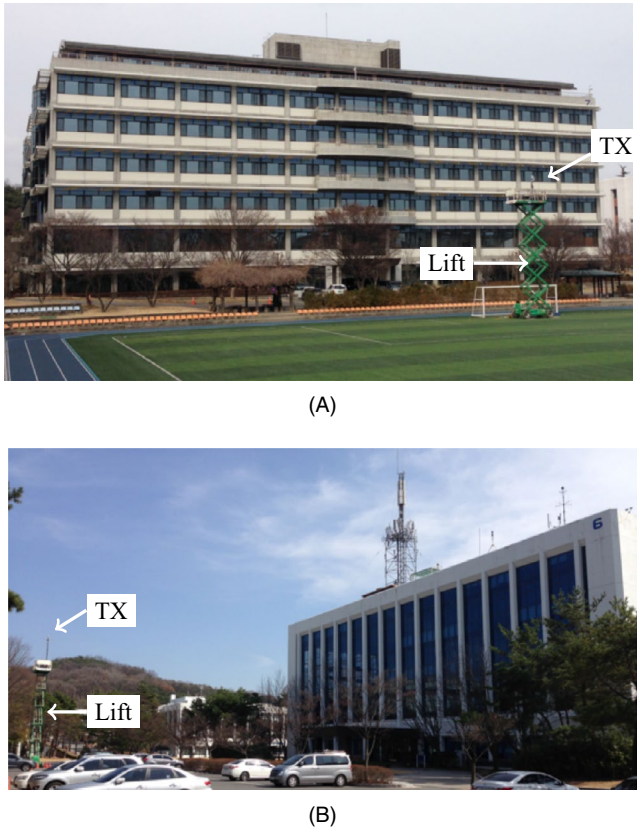

FIGURE 2 Buildings for BEL measurements: (A) Building A and (B) Bulding B

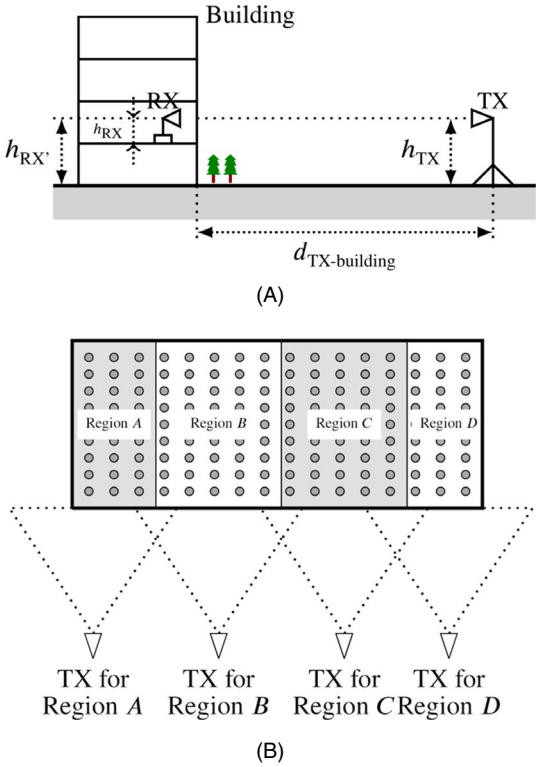

FIGURE 3 BEL measurement setup: (A) Vertical view and (B) horizontal view

from the building to the TX. Figure 3 shows schematic drawings of our measurement setup. In Figure 3A, the antenna heights (from the ground) of the TX and the RX are the same, which is denoted by $h_{TX}(=h_{RX'})$. The distance from the TX antenna to the building facade is denoted by $d_{TX\text{-building}}$. The height of the RX antenna from the floor is denoted by h_{RX}. These parameters are listed in Table 3. As shown in Figure 3B, we tried to collect the RX measurement samples uniformly within the building (actual RX sample points are shown later in Figures 5 and 6, along with the measurement results). Thus, the RX points include various office areas, corridors, computer labs, and conference rooms as shown in Figure 4. At each RX location, an omnidirectional antenna and horn antennas (listed in Table 2) were used for data collections. All the horn antennas were rotated in 10° steps, regardless of the antenna beamwidth. The TX antenna beamwidth (HPBW) was 30°. To consider near-perpendicular incidences on the building facade, we moved the position of TX along with the RX position. As shown in Figure 3B, we divided the measurement area into several regions, and then moved the TX when the region of RX was changed, instead of moving the TX for each individual RX point to save measurement time. While configuring the measurement setup, the vertical and horizontal locations of the TX antenna was aligned with a laser pointer.

4 | MEASUREMENT RESULTS & ANALYSIS

4.1 | BEL measurement data processing

According to the ITU-R guideline in [7], there are two methods for calculating BEL: (a) the excess path loss from the free space loss and (b) the path loss difference from the outside references. Due to security constraints, we were not able to measure the outside reference level; hence, we followed the former method:

$$L_{BEL} = PL_{measurement} - PL_{free}, \tag{16}$$

where $PL_{measurement}$ is the path loss measurement at an indoor RX point and PL_{free} is the relevant free space path loss, that is, $PL_{free} = 20\log_{10}(4\times10^{9}\pi fd/c)$, d is the distance between the TX and the RX, c is the speed of light, and f is the operating frequency in GHz. That is, this BEL measures the additional loss due to the presence of the building (both the exterior and the interior structures). At every RX location, the BEL is calculated with (16) and then statistical tools are applied.

4.2 | Directional and omnidirectional BEL characteristics

Figures 5 and 6 show the BEL measurement results collected with the 10° horn and the omnidirectional antennas, respectively. It can be seen that we have divided five regions for Building A and three regions for Building B, which is heuristically determined by considering the TX distance to the building, the TX antenna beamwidth, and the indoor structure. At each region, the location of TX was fixed at one marked position while the RX was moved to various positions in the region, as illustrated. The direction and length of the arrows

TABLE 3 Measurement configuration

	Building A	Building B
$d_{TX\text{-building}}$ (m)	33	38
$h_{TX}(=h_{RX'})$ (m)	11.7	14.7
h_{RX} (m)	1.5	1.5
# of RX measurement points	79	100

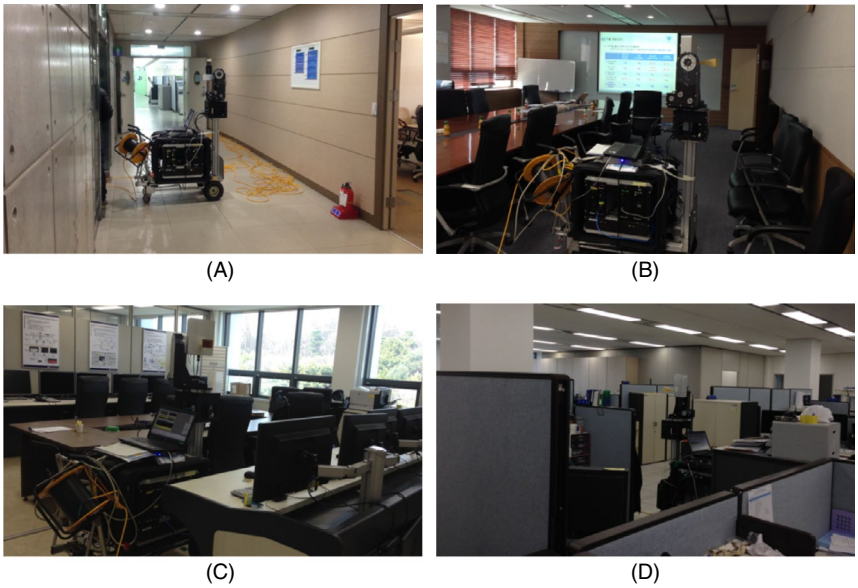

FIGURE 4 Various indoor environments for BEL measurements: (A) Corridor, (B) conference room, (C) computer lab, and (D) open space office

in Figure 5 indicate the direction and strength of the received power, respectively. The color codes illustrate the calculated BEL values. The "×" marks in the figures denote outages. It can be seen that there are many outage points, especially in the omnidirectional measurements (Figure 6). This is due to the small antenna gains (listed in Table 2). Because of the outage issues with the wide beamwidth antenna measurements (not only the omnidirectional antenna but also the 30° and 60° horns), we apply the beam synthesis algorithm [5] to generate the other beamwidth BEL characteristics, while utilizing the un-outaged 30°-horn, 60°-horn, and omnidirectional antenna measurements for beam synthesis calibration.

Figure 7 provides two facts about the directional BEL measurements. First, the variation range of BEL depending on the antenna angle directions is generally large, for example, when the 10°-beamwidth reception is employed, it is 18 dB–46 dB for Building A and 24 dB–53 dB for Building B. Although the variation range decreases as the receive beamwidth increases, variations of more than 20 dB can occur with the 60°-beamwidth reception. This implies the importance of beam alignment when a directional antenna/beamforming is utilized to minimize the building entry loss, even in a multipath-rich indoor environment. Second, the BEL has a strong dependency on the overall propagation loss. As can be seen in Figure 7, the lower ends in the BEL variation range increases as the overall loss increases, which is plausible since the BEL is calculated by the difference between the overall loss and the free space loss as in (16).

4.3 | Beamwidth-dependent directional BEL

As mentioned above, we performed the beamwidth-dependent BEL analysis with the beamwidth-synthesized data from our 10°-horn antenna measurements, which were collected in

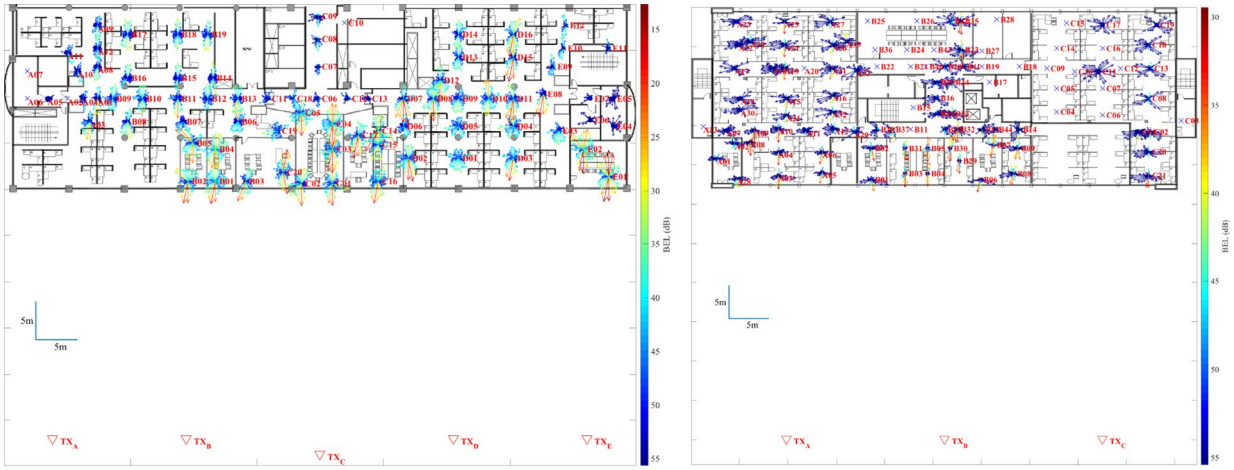

FIGURE 5 BEL measurements with the 10°-horn antenna: (A) Building A and (B) Building B

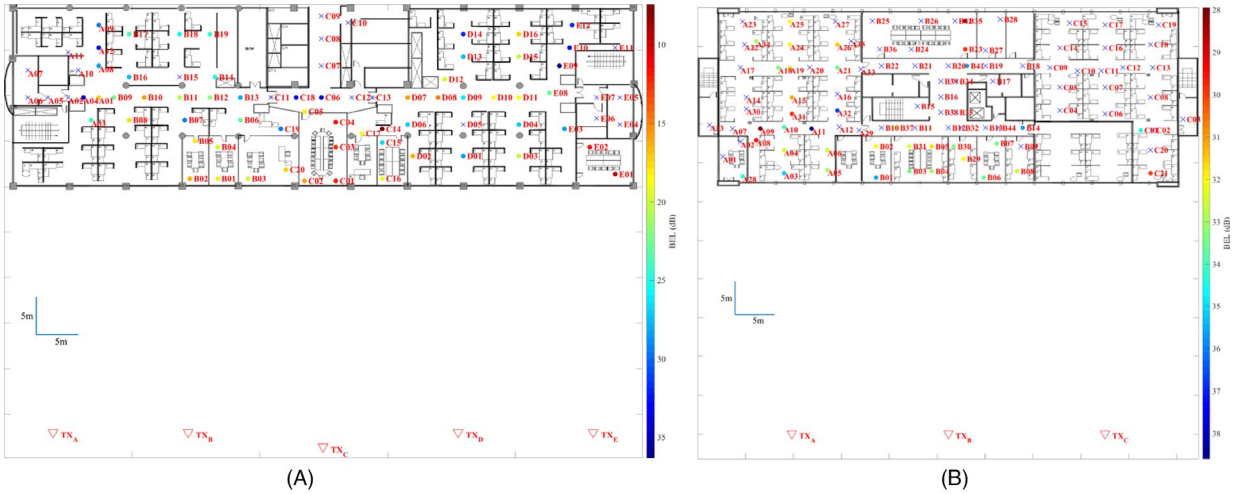

FIGURE 6 BEL measurements with the omnidirectional antenna: (A) Building A and (B) Building B

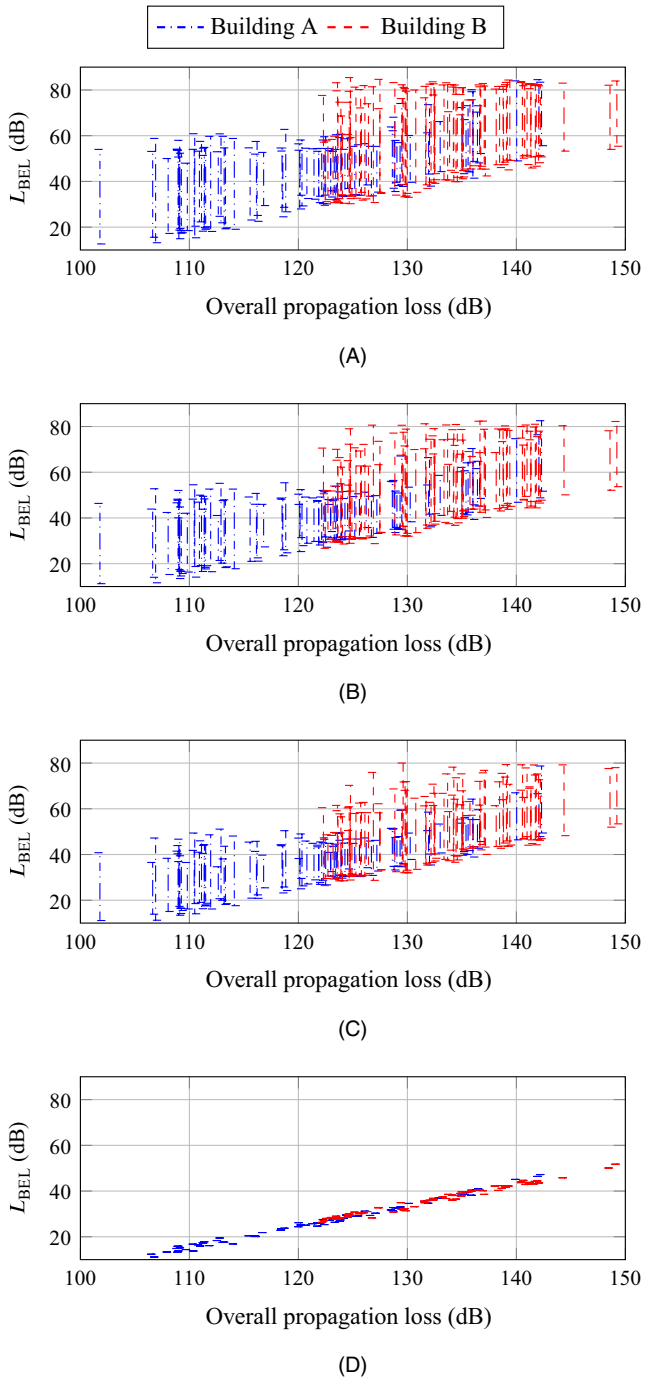

FIGURE 7 BEL variation for various pointing angle directions and the relationship with the overall propagation loss: (A) 10° -beamwidth reception, (B) 30° -beamwidth reception, (C) 60° -beamwidth reception, and (D) omnidirectional reception

10° rotation steps, despite conducting the measurements with several beamwidth antennas such as 10°, 30°, 60° horns, and an omnidirectional antenna (listed in Table 2). This is because the measurement data obtained using the 10°-horn antenna have fewer outage points than the data obtained using the wider-beamwidth antennas. Note that the outage points were assigned to the highest observed loss value to ensure that all the measurement locations are used in the statistical analysis.

We applied the beamwidth-synthesis algorithm in [5] to generate the beamwidth-dependent directional BEL characteristics. One key idea of the beamwidth-synthesis algorithm is the consideration of pointing the antenna boresight to the maximum power direction, which is dependent on the operating beamwidth. Therefore, we re-calculated the boresight direction when the operating beamwidth was varied, that is,

$$\hat{\phi}_{\max} = \arg\max_{\phi} \int_{\varphi=\phi-W_\phi/2}^{\phi+W_\phi/2} P_\varphi, \tag{17}$$

where W_ϕ is the synthesized beamwidth (as described before, this should be in the HPBW) and P_φ is the directional received power in the φ-direction collected with the 10°-horn antenna. With this maximum power direction, the W_ϕ -beamwidth directional received power can be calculated by

$$P_{W_\phi} = \int_{\varphi=\hat{\phi}_{\max}-W_\phi/2}^{\hat{\phi}_{\max}+W_\phi/2} P_\varphi. \tag{18}$$

With this received power, the directional path loss can be calculated using the conventional method of dividing with the transmit power. Since we had actual measurement data obtained using 30° and 60° horns and an omnidirectional antenna, we compared the synthesis data to the actual measurements and observed that the two datasets are in good agreement.

Figure 8 shows the 10°-horn antenna directional BEL and the omnidirectional BEL statistics in comparison with the ITU-R BEL models. It can be seen that the CDFs from our two omnidirectional reception data are generally close to the two ITU-R models, respectively. From this, we infer that our measurement environments (building materials and inside building environments) and the environments in the ITU-R models are in agreement. We can see that the 10°-directional reception data deviate from the omnidirectional reception data for both traditional and thermally efficient buildings. Although we did not explicitly plot the other beamwidth directional reception data (to prevent the graph plots from becoming messy), we observed that the other beamwidth data are monotonic with respect to the beamwidth in between the omnidirectional and 10°-directional data. Thus, the existing ITU-R BEL model does not provide accurate BEL information depending on the antenna beamwidth. To ensure that the median statistics (when the probability is 0.5 in the CDF curves) is more specific, the BEL variation with respect to the antenna beamwidth can be illustrated as in Figure 9. That is, as the antenna beamwidth varies from 10° to omnidirectional, the BEL difference is 5.27 dB and 5.23 dB for Building A and Building B, respectively.

To reflect the narrow antenna beamwidth effect on the ITU-R BEL, we consider the overall beamwidth-dependent directional BEL model as given below:

$$L_{\text{BEL}}^{\text{narrow}}(W_\phi) = L_{\text{BEL}}^{\text{omni}} + \Delta L_{\text{BEL}}(W_\phi)\ (\text{dB}) \tag{19}$$

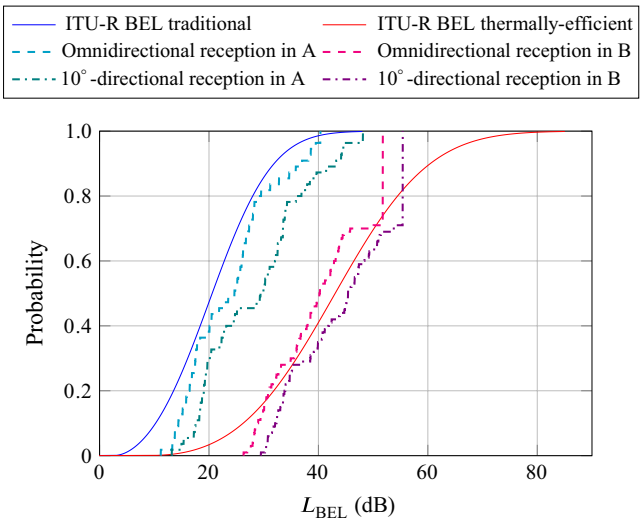

FIGURE 8 Comparison between ITU-R model and measurements

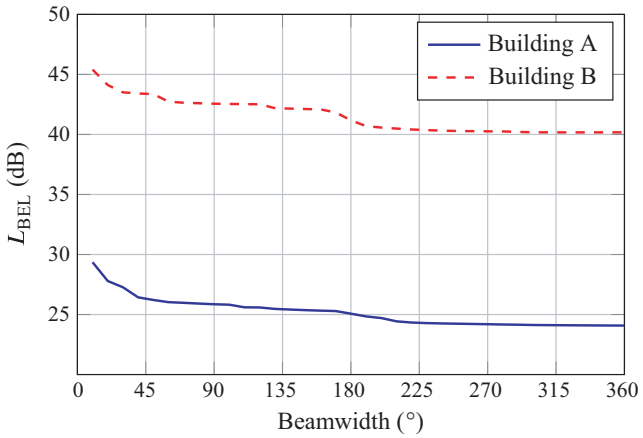

FIGURE 9 BEL variation with respect to antenna beamwidth for $p = 0.5$

where L_{BEL}^{omni} denotes the omnidirectional BEL that can be obtained with the existing ITU-R BEL model in (1) (or the existing 3GPP O2I model in (11)), and ΔL_{BEL} denotes the additional loss due to the antenna beamwidth effect. As we derived the beamwidth-dependent path loss model for outdoor urban environments in [5], we examined our measurement data and found that ΔL_{BEL} is inversely proportional to the beamwidth. By fitting the following model to the measurement data, we obtained the fitting parameter as in Table 4.

$$\Delta L_{BEL}(W_\phi) = \eta\left(\frac{1}{W_\phi} - \frac{1}{360^\circ}\right), \quad 10^\circ \le W_\phi \le 360^\circ. \quad (20)$$

TABLE 4 Constant η for W_ϕ-beamwidth directional BEL

Building	η	RMSE (dB)
A	62.11	1.08
B	54.90	0.86
A & B combined	58.00	0.94

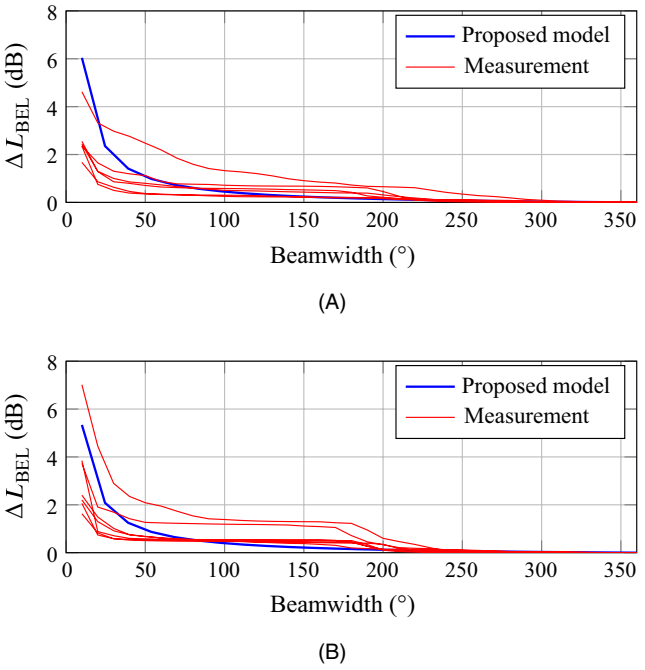

FIGURE 10 Comparison between the measurement data and the model: (A) Building A and (B) Building B

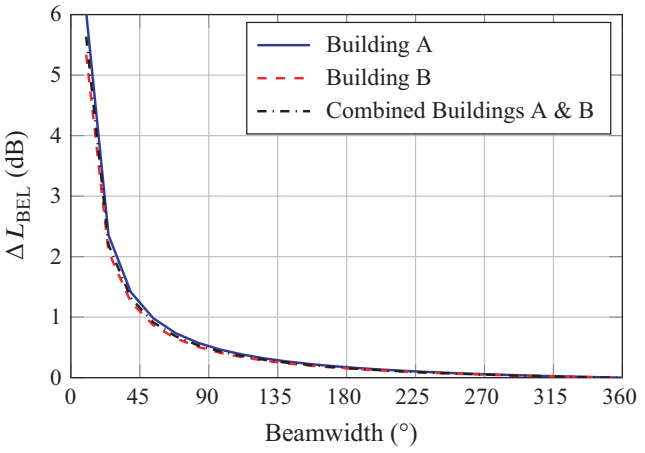

FIGURE 11 Beamwidth effect on the BEL

Figure 10 shows a comparison of the modeling result with the actual measurements for several locations.

As can be seen in Table 4 (as illustrated in Figure 11), the difference in the constant parameter η between Building A and Building B is not significant. This is because the beamwidth effect is relevant to the surrounding indoor environment inside the buildings, whereas L_{BEL}^{omni} captures the building-type differences. That is, the beamwidth-dependent characteristics are relevant to the number of multipaths captured by the corresponding beamwidth antenna (and not by the building type), since the directional gain factor is assumed to be normalized. The captured multipaths are dependent on the surrounding environments of the receiver

(our two selected buildings have similar indoor materials and structures, but different exterior as described before). We obtained a single constant η by simultaneously fitting the measurement data of both Building A and Building B as in Table 4. As can be seen in Figure 11, the combined parameterized model does not deviate substantially from the individually parameterized models.

5 | CONCLUSION

To accommodate a narrow-beamwidth directional beamforming in the omnidirectional-based ITU-R BEL models, we conducted a measurement campaign at two office buildings with various antennas. By analyzing the measurement data, we observed that the directional BEL variations are relatively large, and hence, we realized the importance of accurate beam alignment. We also observed that the BEL statistics are dependent on the antenna beamwidth, regardless of building type. This is more relevant to the indoor environment near the receiver antenna. Both traditional and energy-efficient buildings are modeled together to obtain the beamwidth-dependent BEL behaviors. We believe that this model will provide helpful information on BEL interference evaluation and O2I propagation characteristics when a narrow-beamwidth directional antenna is employed.

ORCID


Juyul Lee https://orcid.org/0000-0002-5851-0615

REFERENCES

1. J. Lee et al., *Empirical investigation of antenna beamwidth effects on the ITU-R building entry loss (BEL) model based on 32 GHz measurements*, in Proc. Global Symp. Millimeter Waves (GSMM), Boulder, CO, USA, May 2018, doi: https://doi.org/10.1109/GSMM.2018.8439686.
2. ITU, Provisional final acts, *The World Radiocommunication Conference (WRC-15): Resolution COM 6/20*, Nov. 2015.
3. Rec. ITU-R P.2109-0, *Prediction of building entry loss*, ITU, June 2017.
4. R. Rudd et al., *The development of the new ITU-R model for building entry loss*, in Proc. Eur. Conf. Antennas Propag., London, UK, Apr. 2018, doi: https://doi.org/10.1049/cp.2018.0720.
5. J. Lee et al., *Field-measurement-based received power analysis for directional beamforming millimeter-wave systems: Effects of beamwidth and beam misalignment*, ETRI J. **40** (2018), no. 1, 26–38.
6. ITU-R Doc 3K/162-E (2017), *Report on the meeting of Working Party 3K*, Working Party 3K Chairman, Geneva, Switzerland, 22–29, Mar. 2017.
7. Rec. ITU-R P.2040-1, *Effects of building materials and structures on radiowave propagation above about 100 MHz*, ITU, July 2015.
8. L. P. Rice. *Radio transmission into buildings at 35 and 150 mc*, Bell Syst. Tech. J. **38** (1959), no. 1, 197–210.
9. C. Oestges et al., *Experimental characterization and modeling of outdoor-to-indoor and indoor-to-indoor distributed channels*, IEEE Trans. Veh. Technol. **59** (2010), no. 5, 2253–2265.
10. H. Okamoto, K. Kitao, S. Ichitsubo. *Outdoor-to-indoor propagation loss prediction in 800-MHz to 8-GHz band for an urban area*, IEEE Trans. Veh. Technol. **58** (2009), no. 3, 1059–1067.
11. S. Wyne et al., *Outdoor-to-indoor office MIMO measurements and analysis at 5.2 GHz*, IEEE Trans. Veh. Technol. **57** (2008), no. 3, 1374–1386.
12. E. Semaan et al., *Outdoor-to-indoor coverage in high frequency bands*, in Proc. IEEE Globecom Conf., Austin, TX, USA, Dec. 2014, pp. 393–398.
13. I. Rodriguez et al., *Radio propagation into modern buildings: Attenuation measurements in the range from 800 MHz to 18 GHz*, in Proc. IEEE Veh. Technol. Conf. (VTC), Vancouver, Canada, Sept. 2014, doi: https://doi.org/10.1109/VTCFall.2014.6966147.
14. T. Imai et al., *Outdoor-to-indoor path loss modeling for 0.8 to 37 GHz band*, in Proc. Eur.Conf. Antennas Propag., Davos, Switzerland, Apr. 2016, doi: https://doi.org/10.1109/EuCAP.2016.7481469.
15. C. Larsson et al., *An outdoor-to-indoor propagation scenario at 28 GHz*, in Proc. Eur. Conf. Antennas. Propag., Hague, Netherlands, Apr. 2014, pp. 3301–3304.
16. H. Zhao et al., *28 GHz millimeter wave cellular communication measurements for reflection and penetration loss in and around building in New York city*, in Proc. IEEE Int. Conf. Commun., Budapest, Hungary, June 2013, pp. 3756–3760.
17. J.-E. Berg. *Building penetration loss along urban street microcells*, in Proc. IEEE Int. Symp. Personal, Indoor Mobile Radio Commun. (PIMRC), Taipei, Taiwan, Oct. 1996, pp. 795–797.
18. COST-231, *Digital mobile radio toward future generation systems*, European Cooperation in Scientific and Technical Research, Bruxelles, 1999.
19. P. Kyosti et al., *WINNER II channel models*, Sept. 2007.
20. J. Meinila et al., *WINNER+ Final Channel Models*, June 2010.
21. GPP TR 38.901, *Study on channel model for frequencies from 0.5 to 100 GHz (release 14)*, Mar. 2017.
22. Rep. ITU-R M.2135-1, *Guidelines for evaluation of radio interface technologies for IMT-Advanced*, Dec. 2009.
23. Rep ITU-R, M.2412-0, *Guidelines for evaluation of radio interface technologies for{IMT-2020*. ITU, Oct. 2017.
24. Rep ITU-R, P.2346-2, *Compilation of measurement data relating to building entry loss*. ITU, Mar. 2017.
25. G. Castro et al., *Outdoor-to-indoor empirical path loss models: Analysis for pico and femto cells in street canyons*, IEEE Wireless Commun. Lett. **6** (2017), no. 4, 542–545.
26. J. Lee et al., *Measurement-based propagation channel characteristics for millimeter-wave 5G giga communication systems*, ETRI J. **38** (2016), no. 6, 1031–1041.

AUTHOR BIOGRAPHIES

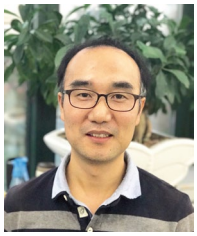

Juyul Lee received his PhD degree in electrical engineering from the University of Minnesota, Twin Cities, USA, in 2010. He was with the Agency for Defense Development, Daejeon, Rep. of Korea from 1998 to 2000. Since 2000, he has been with the Electronics and Telecommunications Research Institute, Daejeon, Rep. of Korea, where he is currently a principal researcher at the Future Mobile Communication Research Division. His research interests include wireless channel modeling, machine learning, and information theory. He has contributed to ITU-R recommendations and reports in Study Group 3 (Propagation) including millimeter-wave propagation models. He is currently the chairman of the ITU-R Correspondence Group 3K-6, which is responsible for studying the impact of higher frequencies (from 6 GHz to 450 GHz) on propagation models and related characteristics.

Kyung-Won Kim received his BS degree in electrical engineering from Korea University, Seoul, Rep. of Korea, in 2009, and his PhD degree in computer and radio communications engineering from Korea university in 2015. Since 2015, he has been with Electronics and Telecommunications Research Institute, Daejeon, Rep. of Korea, where he is currently a senior researcher. His current fields of interest include channel measurement, radio signal processing techniques, channel parameter estimation, and channel modeling.

Myung-Don Kim received his BS and MS degrees in electronics engineering from Dong-A University, Busan, Rep. of Korea, in 1993 and 1995, respectively. Since 1995, he has been with the Electronics and Telecommunications Research Institute, where he is currently a principal researcher at the Future Mobile Research Laboratory. From 2017 to 2018, he was the Director of the Mobile RF Research Section. He is currently a project leader of the Channel Modeling Research Group. His research interests include wireless channel measurements and modelling. Since 2006, he has been involved in many projects for the development of wideband MIMO channel sounder, field measurements, and channel modeling. He has contributed to the development of ITU-R recommendations and reports in Study Group 3 (Propagation), including millimeter-wave propagation models. Since 2014, he has been the chairman of the ITU-R WP3K Draft Group 3K-3A, which studies the prediction methods for short-path outdoor propagation at frequencies from 300 MHz to 100 GHz.

Jae-Joon Park received his BS and MS degrees in control and instrumentation from Chungang University of Seoul, Rep. of Korea in 1997 and 1999, respectively. He is a principal researcher at the Electronics and Telecommunications Research Institute, Daejeon, Rep. of Korea. Since 1999, he has worked on the development of smart antennas for FDD/TDD WCDMA system, the WiBro system for broadband wireless internet services, and wideband wireless channel model for next generation mobile communication. His current research interests include channel modeling for millimeter-wave high-speed vehicular wireless communications.

Young Keun Yoon received his BS degree in electrical engineering from Chungbuk National University, Cheongju, Rep. of Korea, in 1991, and his MS and PhD degrees in radio communication engineering from Chungbuk National University, Cheongju, Rep. of Korea, in 1999 and 2007, respectively. Since 2000, he has been working at the Electronics and Telecommunications Research Institute, Daejeon, Rep. of Korea, where he is now a principal researcher. His main research interests include radio propagation.

Young Jun Chong received his BS degree from the Jeju University, Jeju island, Korea, in 1992, his MS degree in electronics engineering in 1994 from Sogang University, and his PhD degree in Electronic Engineering from Chungnam National University, Daejeon, Korea, in 2005. Since 1994, he has been with ETRI, Daejeon, Korea, where he is a principal member of the research staff of the Radio Technology Department. He is currently involved in the research of spectrum engineering. His research interests include RF circuit and systems. He is a member of KIEES.